JOURNAL OF APPLIED ELECTROCHEMISTRY 24 (1994) 993–1000

Codeposition of SiC powders with nickel in a Watts bath

S. H. YEH

Materials Research Laboratories, Chutung, Hsinchu, Taiwan, ROC

C. C. WAN

Department of Chemical Engineering, Tsing-hua University, Hsinchu, Taiwan, ROC

Received 30 July 1993; revised 28 February 1994

The effect of the silica layer of SiC powder on ionic adsorption was studied in a Watts nickel plating bath. PZC (point of zero charge) measurement suggested that SiC powder has a tendency to release H^+ at pH > PZC (~2.2), and the amount of Ni^{2+} adsorbed on the surface of the SiC increased with increased pH of the Watts bath. Experimental results showed that SiC powders not only catalyzed the adsorption of hydrogen atoms but also had a significant effect on hydrogen evolution during electrodeposition if the solution pH was less than or equal to 2.0 (~PZC). Furthermore, SiC powders have a shielding effect which prevents OH^- from being released into the solution under an applied potential, which results in more $Ni(OH)_2$ in the deposited layer. SiC powders also promote further adsorption of intermediates of nickel on the electrode surface, as shown by impedance studies.

1. Introduction

Composite plating produced by codeposition of powders with a metal has been widely applied to the aerospace, automotive, manufacturing, chemical processing, and hydraulics industries. A composite deposit often has a higher hardness, wear and corrosion resistance.

According to recent literature [1–3], the deposition process commonly involves the following stages:

Stage 1 involves the ionic adsorption of powders which are suspended in an electrolyte. The extent and nature of the adsorbed ions determine the size and magnitude of the charge carried by the powders.

Stage 2 involves the transport process of the solution. Since the mode and intensity of agitation are the determining factors for the powder content in the deposit, improved agitation is helpful in obtaining a better composite layer.

Stage 3 involves loose adsorption between powders and electrode. Loose adsorption is a reversible electrostatic contact, which is closely dependent on the charge size and charge magnitude of the powder, the specific gravity of powder, and the contact time between powder and electrode. High electrolyte velocity can overcome the attractive force of loose adsorption between powder and electrode and can carry the adsorbed powders away from electrode surface.

Stage 4 is a strong adsorption process, which causes the powders to be trapped in the metal matrix. Therefore, the composite deposit is deeply affected by the reduction conditions.

Some workers have endeavoured to make smooth, dense and uniform composite layers by using promoters [4–8], or by increasing the adsorption between powders and electrode [9, 10]. The physical properties of composite layers have also been discussed [11, 12]. Currently, the Ni/SiC composite deposit has applications including the coating of combustion engines and casting moulds. Although there is much discussion about the effects of agitation, current density, and powder content in solution on the codeposition of Ni/SiC [13–15], there has not been a detailed study of ionic adsorption in a Watts bath from the standpoint of PZC [16]. PZC means that the suspended solution is kept at a pH, which makes the surface charge of SiC powder equal to zero. In this work, the effect of pH on the codeposition mechanism of Ni/SiC has been studied by changing the pH of the Watts baths away from the PZC of SiC powder and the behaviour of electrodeposited nickel with or without SiC powders has been examined.

2. Experimental details

α-SiC powders with specific gravity of 3.2 and over 99% purity were used in this experiment. The surface area was about $11.0\,m^2\,g^{-1}$ and the particle size approximately $1.5 \sim 1.6\,\mu m$. The surface binding state of the composite deposit was measured by ESCA (Electron Spectroscopy for Chemical Analysis). The surface charge of the SiC powders in NaCl electrolytes was estimated by potentiometric titration [17], and the zeta potential was calculated from streaming potential data [7].

All chemicals used were EP grade. The basic composition of the Watts bath was $NiSO_4 \cdot 6H_2O$ 1.33 M, $NiCl_2 \cdot 6H_2O$ 0.19 M, H_3BO_3 0.57 M and H_2SO_4 was used to adjust pH.

To keep the SiC powders in a homogeneous suspension, a magnetic stirrer was used for two days before

0021-891X

measurement. The current efficiency of the deposited layer was calculated as $Q_{Ni}/Q_{tot} \times 100$, where Q_{Ni} is the real charge estimated from the quantity of deposited nickel and Q_{tot} is the theoretical charge calculated by Faraday's law.

The amount of H^+ adsorbed on the SiC surface may be evaluated from the pH change. This represents the difference between the pH of the suspended solution is obtained after prolonged settlement and the pH of the initial solution without SiC powder. In addition, the quantity of Ni^{2+} adsorbed on the surface of SiC powder was analysed by ICP–AES (inductively coupled plasma–atomic emission spectrometer).

A Potentiostat (EG & G Parc Model 273) was connected to the rotating disc electrode (EG & G Parc Model 616). The working electrode was a platinum disc 0.5 cm in diameter, which had been predeposited with 3 μm nickel. The reference electrode was a Ag/AgCl electrode (Ingold Company) and the counter electrode was a platinum plate of 99.9% purity. The potentiostat was connected to a lock-in amplifier (EG & G Parc Model 5210) for the a.c. impedance study. The frequency range was from 0.001 Hz to 100 kHz, the amplitude 10 mV, and the applied potential was controlled below −750 mV to electrodeposit nickel.

Finally, scanning electron microscopy was applied to study the powder distribution and content.

3. Results and discussion

3.1. *SiC surface chemistry*

Figure 1 shows the surface state of SiC powders analysed by ESCA. Si, C and large quantities of O appear in the spectrum shown in Fig. 1(a) and the two peaks have a net difference of about 3 eV (102.9 eV and 106.0 eV) in the microscan spectrum of Si_{2p} shown in Fig. 1(b). The two peaks of Fig. 1(b) represent SiC and SiO [18, 19], respectively, and the SiO structure (silica layer) is attributed to the fact that the adsorbed oxygen chemically reacts with SiC. A high peak of O resulted from both chemical and physical adsorption of oxygen at the same time. In fact, Rahaman [20] observed that the SiC surface had a silica layer of about 3 ~ 5 nm, and Chassaing *et al.* [21] also found that the hydration of the silica layer would transfer to 4.5 sites nm^{-2} Si–OH in the aqueous solution. These cases obviously match our result.

3.2. *Cation adsorption*

Figure 2 shows the surface charge of SiC in the NaCl electrolytes at various pH levels. It is found that SiC powders have positive surface charge at pH < 2.2 and negative surface charge at pH > 2.2. pH 2.2 is therefore the PZC. In addition, surface charge obviously increases as the pH decreases. This is owing to the fact that SiC powders have a strong tendency to adsorb H^+ at the lower pH levels. Figure 3 shows that the zeta potential is also zero at pH around 2.2. This means that the IEP (isotropic electrical point) of SiC is at pH 2.2 in this case. Consequently, because of PZC of SiC at pH around 2.2 is similar to the PZC of SiO_2 at pH around 2 [22], a silica layer which has been formed on the surface of the SiC powder is again confirmed. In addition, since the PZC of SiC is the same as the IEP in NaCl electrolyte, Na^+ and Cl^- are non-specific adsorbed ions for the SiC powders.

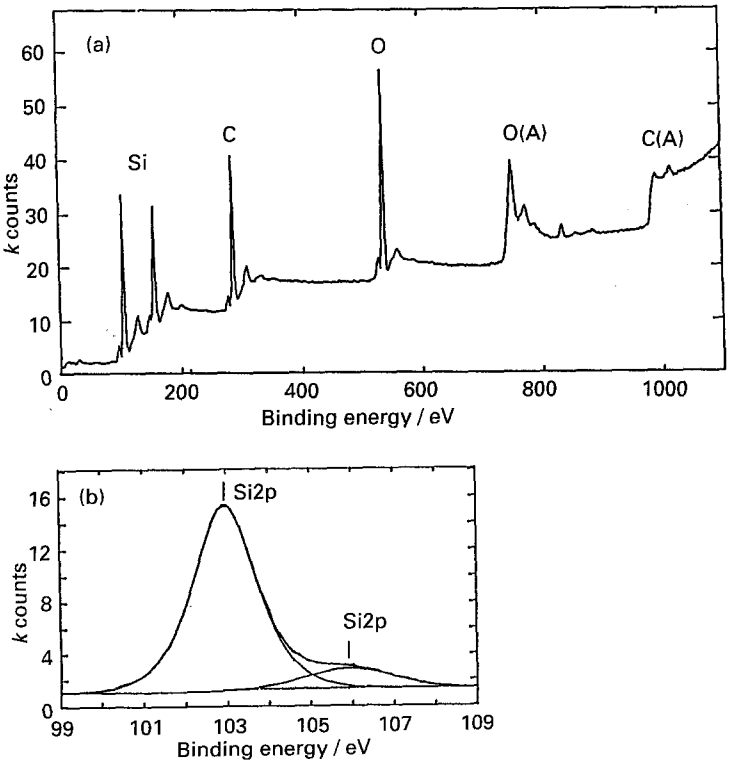

Fig. 1. Analysis of SiC powders using ESCA: (a) Survey spectrum; (b) spectrum of Si_{2p} (peaks exist at 102.9 eV and 106.0 eV). (MgK_α radiation, 500 eV analyser, step size 1.0 eV).

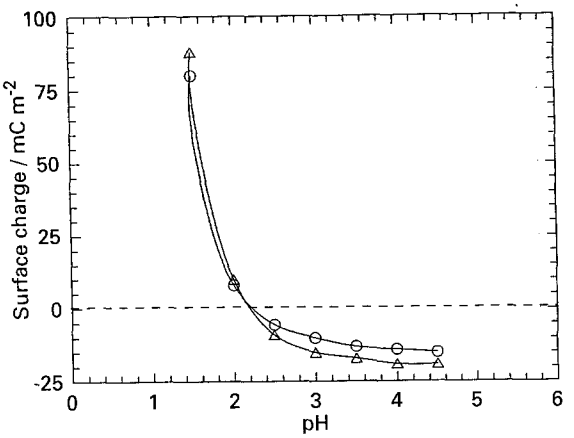

Fig. 2. Surface charge of SiC powders in (○—○) 0.01 M and (△—△) 0.05 M NaCl electrolyte.

A two-site model was introduced by Levine and Smith [23] to describe the behaviour of the oxide/solution interface and has been further modified by Yates *et al.* [24]. This model can be used to demonstrate the acceptance or release of a proton by the silanol group of the silica layer in aqueous solution.

$$SiOH + H_2O \overset{K_1}{\rightleftharpoons} SiOH_2^+ + OH^- \quad (1)$$

$$SiOH + H_2O \overset{K_2}{\rightleftharpoons} SiO^- + H_3O^+ \quad (2)$$

so that

$$pK_1 = pH + \log([SiOH_2^+]/[SiOH]) \quad (3)$$

$$pK_2 = pH + \log([SiOH]/[SiO^-]) \quad (4)$$

where $pK_1 \sim -2.77$ and $pK_2 \sim 6.87$ [25] and $PZC = (pK_1 + pK_2)/2$.

In fact, $SiOH_2^+$ and SiO^- do not exist alone in the solution. They generally combine with other counter-ions to balance the surface charge of these powders.

Figure 4 shows that the pH change (final pH – initial pH) is negative after 5.88% SiC powder has been added to solution when the initial pH is greater than 2.0 (~PZC), but it is marginal when the initial pH is less than 2.0. The pH change is negative due to the fact that the silanol group of SiC powders releases H^+ into solution according to Equation 2, if

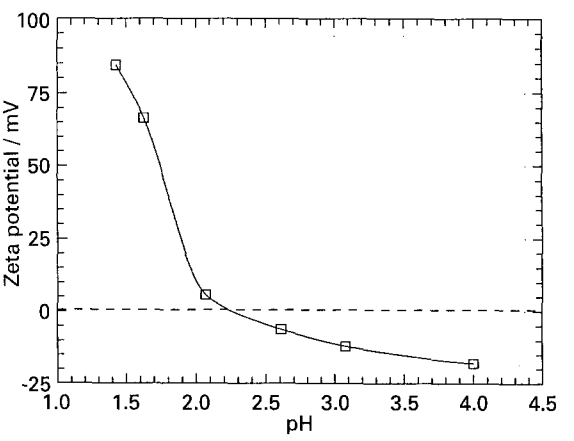

Fig. 3. Zeta potential of SiC powders in 0.01 M NaCl supporting electrolyte at different pHs.

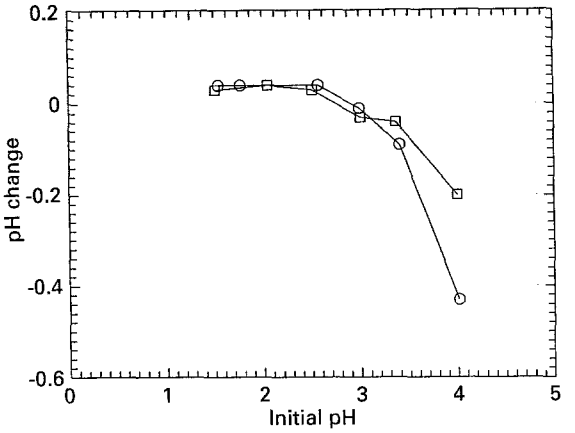

Fig. 4. pH change after 5.88% SiC powders were added to the solution without (○—○) or with (□—□) $NiSO_4$ at different initial pHs.

the initial pH ⩾ PZC. However, there is not much difference between the initial and final pH if the initial pH < ~ 2.0. This is because the concentration of H^+ is too high to be adsorbed completely by the SiC powders.

The net pH change decreases as the solution contains $NiSO_4$. One possible reason is that an exchange reaction occurs with $NiSO_4$, which can be expressed as,

$$-SiOH + Ni^{2+} \rightleftharpoons -SiO^-Ni^{2+} + H^+ \quad (5)$$

Ni^{2+} tends to balance SiO^- and decreases the dissociation of H^+.

Figure 5 shows that the quantity of Ni^{2+} adsorbed on the SiC surface increases as initial pH increases. The degree of absorption appears to be proportional to the amount of SiO^- dissociated from the silica layer.

3.3. *ESCA analysis*

In order to understand the reaction mechanism during nickel electrodeposition, nickel deposits with or without SiC powder were analysed by ESCA at the applied potential of −700 mV or −750 mV.

Figure 6 shows that there are two peaks at 852.8 eV and 856.3 eV, respectively, which represent Ni and

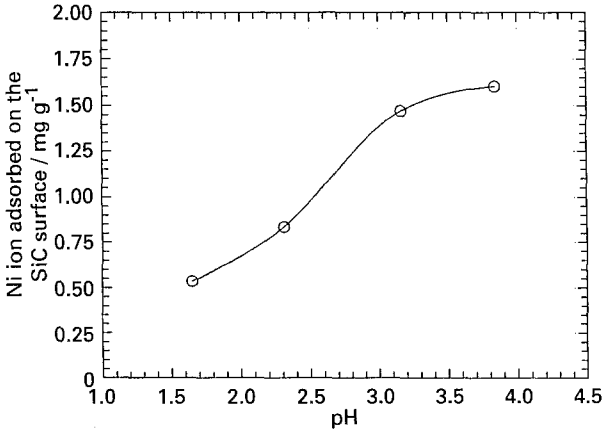

Fig. 5. Quantities of Ni^{2+} adsorbed on the SiC powders surface in a solution with only one tenth of the concentration of Watts bath.

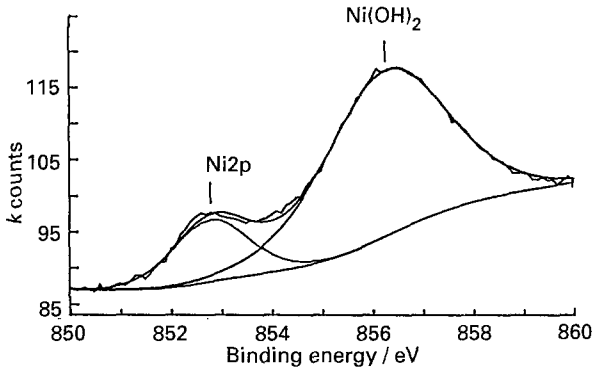

Fig. 6. ESCA analysis of electrodeposited layer produced in the Watts bath at pH 4.00 and −700 mV vs Ag/AgCl. (MgK_α radiation, 500 eV analyser, step size 1.0 eV).

$Ni(OH)_2$ [26]. The area ratios of the $Ni(OH)_2$ peak to the Ni peak are summarized in Table 1. This ratio increases if the solution contains SiC powder, and decreases when the applied potential decreases. It is well-known that both nickel and hydrogen reduction occur in the Watts bath. In this case the hydrogen evolution happens on the surface of the electrode and increases the local pH near the electrode at −750 mV or −700 mV. Therefore, if the solution contains SiC powder during nickel electrodeposition, the powders on the electrode will hinder the OH^- group generated from the hydrogen evolution from being released into the solution. This process also results in more $Ni(OH)_2$ in the deposit. In addition, because the amount of hydrogen evolution decreases as the applied potential decreases, the quantity of $Ni(OH)_2$ in the deposit also decreases at a lower potential.

3.4. *Impedance study*

Impedance measurements allow the elementary steps of an electrochemical reaction to be separated on the basis of different relaxation time constants. Therefore, the kinetics of nickel electrodeposition were studied by the impedance technique. Figure 7(a) shows that there exist two semicircles in the Nyquist plots. This shows that two consecutive electron transfer reactions occur during the reduction. The capacitive loop, which exists in the high frequency

Table 1. Peak ratio of $Ni(OH)_2/Ni$
Peak area of ESCA spectrum for electrodeposited layer analysed by curve fitting of Gauss distribution

Conditions			*Peak ratio of* $Ni(OH)_2/Ni$
pH	SiC	V^*_{app}/mV	
4.00	without	−750	1.9
4.00	with	−750	5.8
4.00	with	−700	4.3
1.65	without	−750	2.6
1.65	with	−750	5.7

* V_{app} represents that applied potential against Ag/AgCl

range (100 kHz ~ 10 Hz), represents the double layer capacitance, and the inductive loop, which appears in the lower frequency (< 10 Hz), is produced by the adsorbed intermediate [27] on the electrode surface.

During nickel electrodeposition, the intermediate of Ni^+_{ads} is involved in the mechanism as described [28–30] below:

$$2H^+ + 2e^- \longrightarrow H_2 \quad (6)$$

$$Ni^{2+} + e^- \longrightarrow Ni^+_{ads} \quad (7)$$

$$Ni^+_{ads} + e^- \longrightarrow Ni \quad (8)$$

$$Ni^{2+} + Ni^+_{ads} + 2e^- \longrightarrow Ni^+_{ads} + Ni \quad (9)$$

$$H^+ + Ni^+_{ads} + e^- \longrightarrow Ni^+_{ads} + H_{ads} \quad (10)$$

$$Ni^+_{ads} + H_{ads} \longrightarrow Ni + H_{include} \quad (11)$$

Ni^+_{ads} is more or less solvated and possibly complexed as $NiOH_{ads}$, which was proposed as an intermediate in pure nickel plating or dissolution processes [31–33]. Consequently, the semicircle shown in the lower frequency range of Fig. 7(a) is regarded as due to Ni^+_{ads}, an adsorbed intermediate, being produced on the electrode.

Figure 7(b) shows the Nyquist plots of the Watts bath with SiC powder at various pH. The main difference between Fig. 7(a) and (b) is that the semicircle which appears in either the low or high frequency range becomes much smaller at pH ⩽ 2.0 (~ PZC) when the solution contains SiC powder. It seems that the reduction paths of Ni^+_{ads} change if

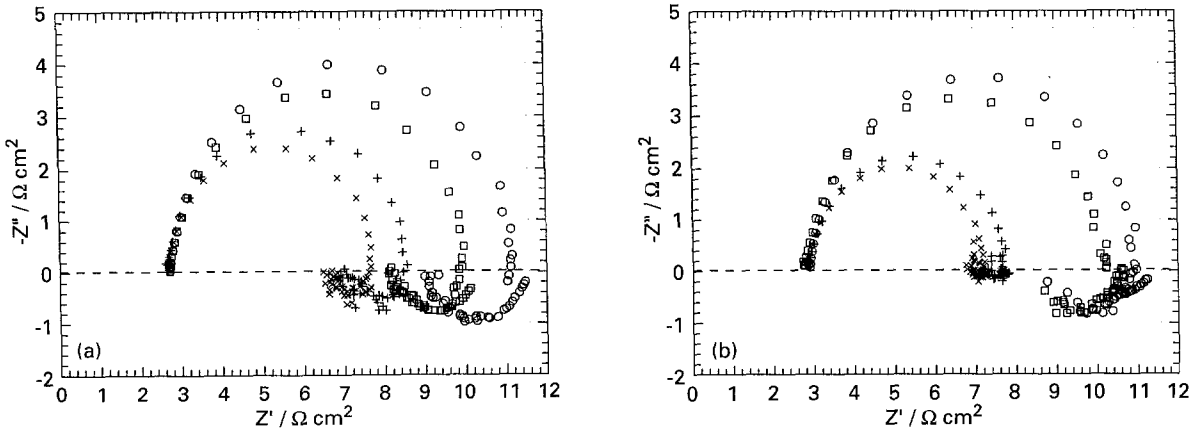

Fig. 7. Nyquist plots of electrodeposited nickel in the Watts bath at −750 mV vs Ag/AgCl and various pHs (a) without SiC; (b) with SiC. Key: pH (○) 4.00, (□) 3.00, (+) 2.00 and (×) 1.65.

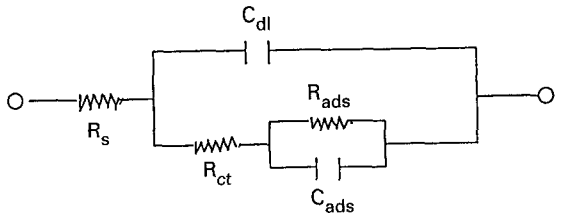

Fig. 8. An equivalent circuit describes the schematic of electrochemical reaction of nickel plating.

the solution contains SiC and the adsorbed H^+ on the SiC surface may also participate in the nickel electrodeposition.

The impedance studies suggest that nickel electrodeposition with or without SiC powders is a multistep reaction, including a charge transfer reaction which produces the adsorbed intermediate and a subsequent consumption reaction with the adsorbed intermediate. Figure 8 shows the equivalent circuit [27] representing the electrochemical behaviour of electrodeposited nickel. In this circuit, R_s represents the solution resistance, R_{ct} the charge transfer resistance, C_{dl} the double layer capacitance, C_{ads} the pseudocapacitance from the adsorbed intermediates and R_{ads} desorption resistance. C_{ads} and R_{ads} are often used to account for the surface coverage of the adsorbed intermediates and the rate of desorption.

The simulation results of the circuit for the Watts bath with SiC powder at pH 4.00 are shown in Fig. 9, giving the following values: $R_s \sim 14.7\,\Omega$, $R_{ct} \sim 39.0\,\Omega$, $C_{dl} \sim 8.6\,\mu F\,cm^{-2}$, $R_{ads} \sim 8.4\,\Omega$, $C_{ads} \sim 90270\,\mu F\,cm^{-2}$, τ_H $(= C_{dl}R_{ct}) \sim 0.34$ ms and τ_L $(= C_{ads}R_{ads}) \sim 910$ ms. Because $\tau_H \ll \tau_L$, the reaction of intermediates is the rate determining step during nickel electrodeposition. A series of simulation results at different pH values may be summarized as follows.

Table 2 shows that most of R_{ct} in the solution with SiC is higher than that without SiC at pH $\geqslant$ 3.0. From Figs 4 and 5, we learn that SiC powders have a tendency to adsorb more Ni^{2+} in the form of SiO^-Ni^{2+} at high pH and to adsorb more H^+ in the form of $SiOH_2^+SO_4^{2-}$, or $SiOH_2^+Cl^-$ at low pH. Therefore, at pH $\geqslant$ 3.0, the adsorbed SiO^-Ni^{2+} on SiC surface is probably reduced to a form of $SiONi_{ads}$,

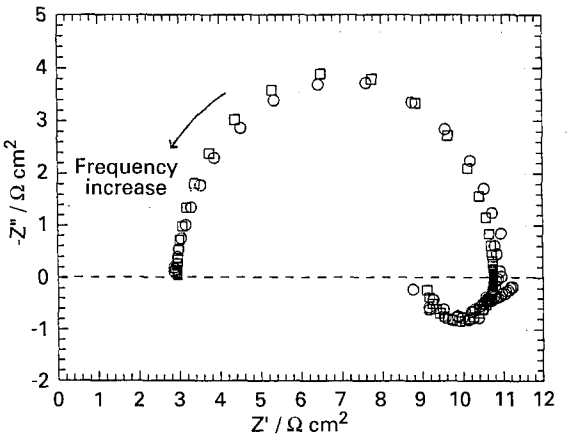

Fig. 9. A comparison of Nyquist plot of the simulation (□) values with the measured (○) data of Fig. 7(a) at pH 4.00.

Table 2. Charge transfer resistance

V_{app}/mV	*pH*	R_{ct}/Ω	
		without SiC	*with SiC*
−750	4.00	39.0 ± 0.6	39.0 ± 0.3
	3.00	35.9 ± 0.4	37.6 ± 1.0
	2.50	32.7 ± 0.3	30.1 ± 0.3
	2.00	28.5 ± 0.4	23.7 ± 0.2
	1.65	24.6 ± 0.3	21.5 ± 0.2
−700	4.00	84.1 ± 0.6	96.0 ± 0.9
	3.00	74.7 ± 0.6	80.0 ± 0.8
	2.50	71.9 ± 0.7	58.0 ± 0.4
	1.65	53.2 ± 0.7	39.8 ± 0.2
−650	4.00	231.1 ± 1.8	230.0 ± 2.8
	3.00	163.8 ± 1.3	193.3 ± 3.1

which is understandably more difficult than the direct reduction of Ni^{2+} to Ni^+_{ads} from the solution without SiC powder. In addition, the actual active surface area of electrode may decrease by the adsorbed SiC powder. All these contribute to an increase of R_{ct} when the solution has SiC powder at pH $\geqslant$ 3.0 during electrodeposition of nickel. Whereas, at pH < 3.0, the R_{ct} for system with SiC becomes smaller than that without SiC as shown in Table 2. This is because the adsorbed H^+ on the SiC surface increases with decreased pH, and the increased H^+ near the electrode reduce the overpotential of reduction. The increased amount of adsorbed H^+ near electrode can also result in increased hydrogen evolution, which repels the contact of powders with the electrode and decreases the shielding effect of adsorbed powders. Hence R_{ct} decreases with decreased pH at pH < 3 in the presence of SiC powder.

Obviously, SiC powder not only catalyse hydrogen evolution but also change the reduction paths during nickel electrodeposition.

The main differences among Fig. 10(a)–(d) are that Fig. 10(c) and (d) have a capacitive loop which appears in the lowest frequency range for the system with SiC at pH $\leqslant$ 2.0 (~ PZC). The capacitive loop, which appears in the lowest frequency, is caused by hydrogen discharge, as also discussed by Epelboin *et al.* [29] in $NiSO_4$ or $NiCl_2$ electrolytes without SiC powder. Therefore, a possible mechanism to explain this capacitive loop is

$$SiOH_2^+ + Ni^+_{ads} + e^- \longrightarrow Ni^+_{ads} + SiOH + H_{ads} \quad (12)$$

$$SiOH_2^+ + H_{ads} + e^- \longrightarrow SiOH + H_2 \quad (13)$$

$$H_{ads} + H_{ads} \longrightarrow H_2 \quad (14)$$

Equations 13 and 14 represent H_2 evolution by electrochemical and chemical desorption in the presence of H_{ads}. The fact that H_{ads} appears in the lowest frequency range proves that SiC powder is a medium for H^+ transfer as indicated in Equation 12 and 13 and can enhance hydrogen evolution at a lower pH.

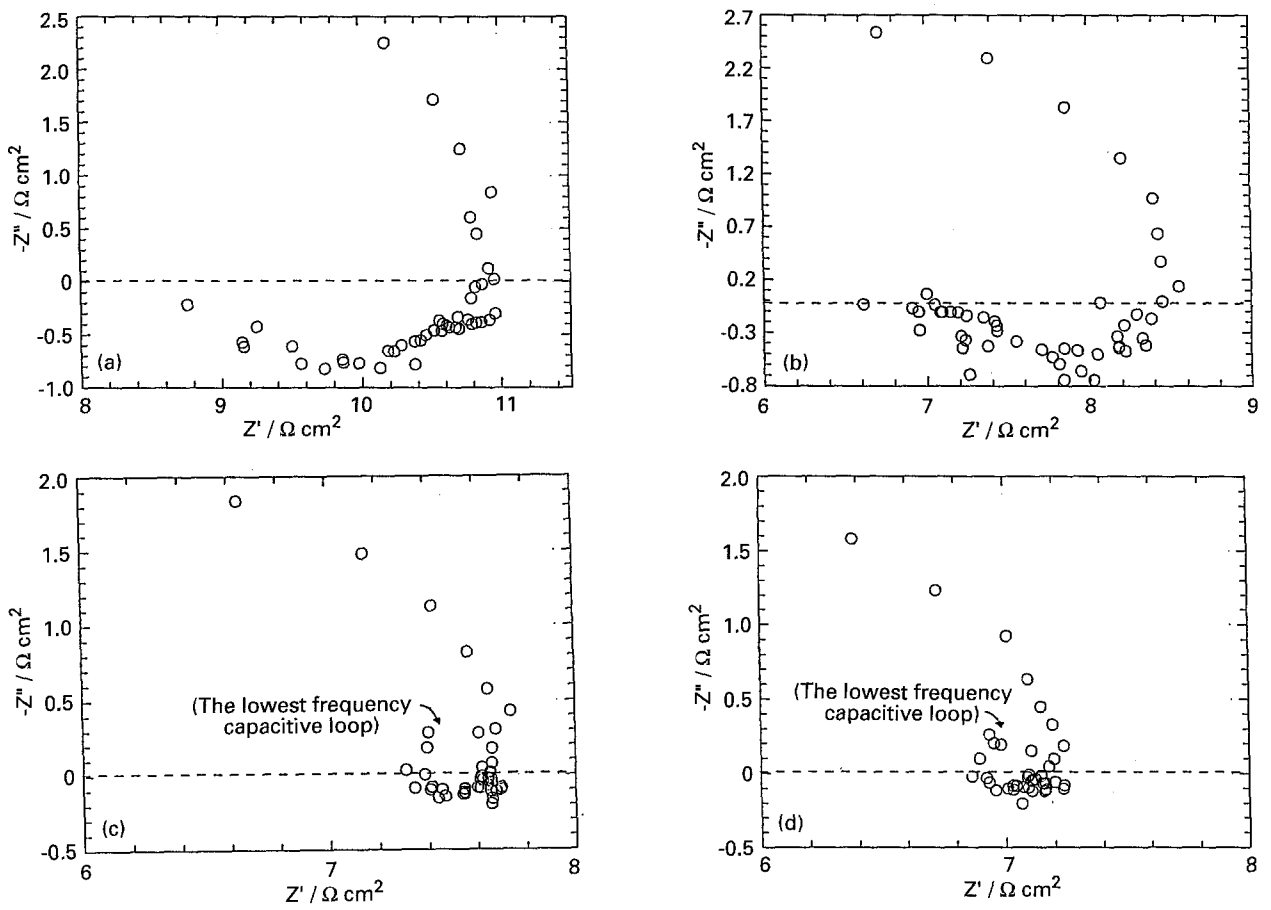

Fig. 10. Nyquist plots of lower frequency of electrodeposited nickel at −750 mV vs Ag/AgCl: (a) pH 4.00, with SiC; (b) pH 2.00, without SiC; (c) pH 2.00, with SiC; (d) pH 1.65, with SiC.

Table 3 shows that C_{ads} for the system with SiC is much larger than that without SiC. Probably, the occupied area of Ni^{+}_{ads} increases with the addition of SiC powder. The only possible places where the increased intermediates exist are on the powder surface near the electrode. The adsorbed intermediates probably exist as $SiONi_{ads}$. These $SiONi_{ads}$ and Ni_{ads} on the electrode surface result in a larger C_{ads}. In addition, we find that C_{ads} decreases with decreased pH in a solution with or without SiC powder as indicated in Table 3. This is owing to the fact that increased H^{+} easily react with Ni^{+}_{ads}, by following Equations 10 and 11.

Table 3. Pseudocapacitance

V_{app}/mV	pH	$C_{ads}/\mu F\,cm^{-2}$	
		without SiC	*with SiC*
−750	4.00	31870 ± 6300	90270 ± 13130
	3.00	23290 ± 3800	128100 ± 20000
	2.50	21800 ± 600	111700 ± 25700
	2.00	19660 ± 3620	103600 ± 4500
	1.65	19860 ± 3870	N*
−700	4.00	18400 ± 1830	482300 ± 66850
	3.00	14780 ± 1460	822100 ± 134660
	2.50	11130 ± 1320	124000 ± 15400
	1.65	7800 ± 1240	N*
−650	4.00	17150 ± 2050	77870 ± 11630
	3.00	21580 ± 2370	96780 ± 15600

* N: Data is not obtainable from analysis.

3.5. *Current efficiency and powders content*

Figure 11 shows that current efficiency (CE) in general increases as pH increases. However, the CE for systems with SiC is lower than that without SiC at the same current density. It is again consistent with the reasoning that SiC powders carry more H^{+} to

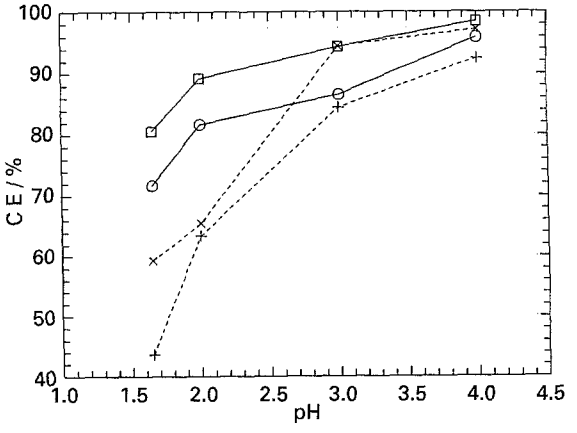

Fig. 11. A comparison of current efficiency of nickel electrodeposition between the Watts bath with 2.48% SiC powders and that without SiC powders. (○—○) 24 mA cm^{-2} without SiC; (□—□) 16 mA cm^{-2} without SiC; (+——+) 24 mA cm^{-2} with SiC; (×——×) 16 mA cm^{-2} with SiC.

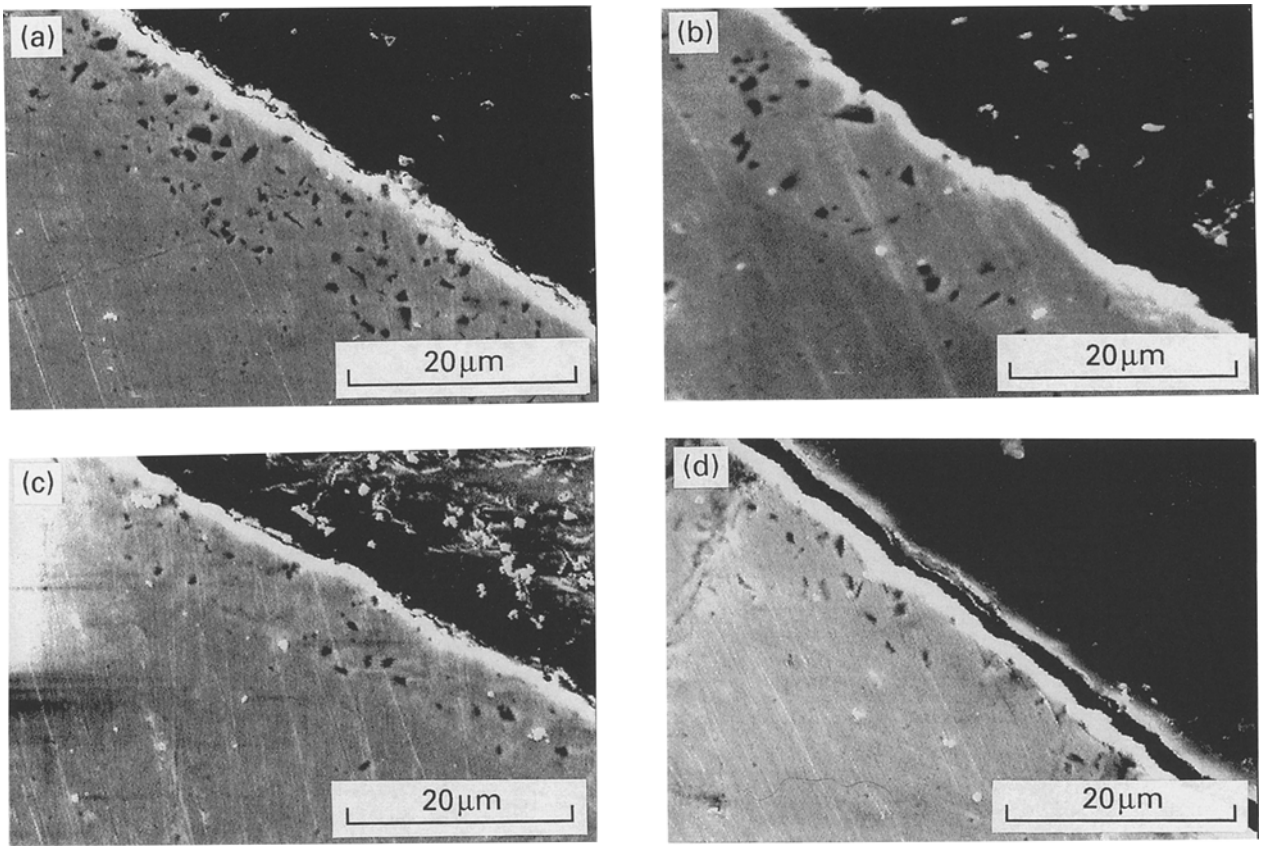

Fig. 12. SEM pictures of cross section of nickel deposit produced in the Watts bath with 2.48% SiC powders at current density 16 mA cm^{-2} (a) pH 4.00; (b) pH 3.00; (c) pH 2.00; (d) pH 1.65.

enhance the hydrogen evolution at pH less than 2.0 and carry few H^+ ions at pH $3 \sim 4$ which account for very little difference of current efficiency between solutions with and without SiC powders. These results suggest that cation adsorption behaviour is controlled by the PZC and affects the nickel electrodeposition current efficiency.

Figure 12 shows that the quantity of SiC powder in the deposit layer decreases as pH decreases. This is because hydrogen evolution removes the loosely adsorbed SiC powders and decreases the amount of SiC powder codeposited with nickel. Therefore, in solutions with too low pH it is difficult to obtain a dense composite layer containing sufficient powder.

4. Conclusions

It has been verified that there exists a silica layer on the surface of SiC powders, and a silanol group dissociates from this layer. It has also been found that the PZC of SiC powders is about 2.2, which is responsible for the dissociation ratio of $[SiO^-]/[SiOH_2^+]$. In addition, SiC powders release H^+ into bulk solution at solution pH > 2.0 ($\sim$ PZC) and adsorb more Ni^{2+} at high pH than at low pH.

SiC powder not only increases the concentration of reductant near the local contact area but also produce a shielding effect on the active surface during electrodeposition. SiC powders prevent OH^- from releasing into bulk solution, which results in more $Ni(OH)_2$ in the deposited layer.

From the results of the impedance study, it was found that SiC powder promotes more area for the adsorption of Ni^+_{ads} intermediate which is in the form of $SiONi_{ads}$ on the SiC surface near the electrode, and $SiONi_{ads}$ causes an increase in C_{ads}. In addition, SiC powders catalyse H_{ads} and enhance hydrogen evolution at pH $\leqslant 2.0$ ($\sim$ PZC). Therefore, the powder content in the deposited layer and the current efficiency both decrease with decreasing pH in the Ni/SiC codeposition system.

Acknowledgement

The authors thank the Ministry of Economic Affairs of the Republic of China for financial support.

References

[1] J. Zahavi and J. Hazan, *Met. Fin.* **81** (Feb. 1983) 57.
[2] J. P. Celis, J. R. Roos and C. Buelens, *J. Electrochem. Soc.* **134** (1987) 1402.
[3] J. W. Graydon and D. W. Kirk, *ibid.* **137** (1990) 2062.
[4] J. R. Roos, J. P. Celis and J. A. Helsen, *Trans. IMF* **55** (1977) 113
[5] J. R. Roos, H. Kelchtermans and J. R. Roos, *ibid.* **56** (1978) 41.
[6] T. W. Tomaszewski, *ibid.* **54** (1976) 54.
[7] D. W. Snaith and P. D. Groves, *ibid.* **56** (1978) 9.
[8] C. C. Lee and C. C. Wan, *J. Electrochem. Soc.* **135** (1988) 1930.
[9] N. Guglelmi, *ibid.* **119** (1972) 1009.
[10] Y. Suzuki and O. Asai, *ibid.* **134** (1987) 1905.
[11] M. Ghouse, *Met. Fin.* **82** (Mar. 1984) 33.
[12] M. Thoma, *ibid.* **82** (Sep. 1984) 33.

[13] V. P. Greco, *Plat. Surf. Fin.* **76** (July 1989) 62.
[14] J. Sadowska-Mazur, M. E. Warwick and R. Walker, *Trans. IMF* **64** (1986) 142.
[15] G. N. K. Ramesh Bapu, J. Ayyapparaju, R. Mahalingam, G. Devaraj and S. Guruviah, *B. Electrochem.* **6** (Feb. 1990) 245.
[16] A. J. Bard and L. R. Faulkner, 'Electrochemical methods', Wiley, New York (1980) pp. 511–515.
[17] R. Sprycha, *Colloids Surf.* **5** (1982) 147.
[18] R. B. Shalvoy, P. J. Reucroft and B. H. Davis, *J. Catal.* **56** (1979) 366.
[19] T. L. Barr, *Appl. Surf. Sci.* **15** (1983) 1.
[20] M. Rahaman, Y. Boiteux and C. De Jonghe, *Am. Ceramic Soc. Bull.* **65** (1986) 1171.
[21] E. Chassaing, M. Joussellin and R. Wiart, *J. Electroanal. Chem.* **157** (1983) 75.
[22] J. C. Bolger, 'Adhesion Aspects of Polymeric Coatings', New York, London (1983) pp. 3–5.
[23] S. Levine and A. L. Smith, *Disc. Faraday Soc.* **52** (1971) 290.
[24] D. E. Yates, S. Levine and T. W. Healy, *J. Chem. Soc. Faraday* **70** (1974) 1807.
[25] W. H. Morrison, *J. Coat. Tech.* **57** (1985) 55.
[26] N. S. McIntyre, T. E. Rummery, M. G. Cook and D. Owen, *J. Electrochem. Soc.* **123** (1976) 1164.
[27] S. W. Watson and R. P. Waiters, *ibid.* **138** (1981) 3633.
[28] I. Epelboin and R. Wiart, *ibid.* **118** (1971) 1577.
[29] I. Epelboin, M. Joussellin and R. Wiart, *J. Electroanal. Chem.* **119** (1981) 61.
[30] E. Chassaing, M. Jousellin and R. Wiart, *ibid.* **157** (1983) 75.
[31] J. Matulis and R. Slizys, *Electrochim. Acta* **9** (1964) 1177.
[32] K. E. Heusler and L. Gaisr, *ibid.* **14** (1969) 541.
[33] R. C. V. Piatti, A. J. Ariva and J. J. Podesta, *ibid.* **98** (1975) 161.